钢箱梁焊接接头的断裂韧度评定

苗张木[1]， 吴 卫国[1]， 陶得馨[2]， 谢智华[3]

（1. 武汉理工大学 交通学院，武汉 430063； 2. 武汉理工大学 物流学院，武汉 430063；
3. 中铁大桥局集团第七工程公司，江西 九江 332004）

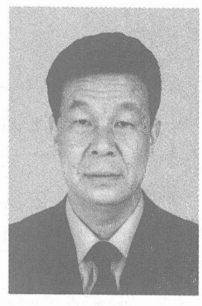

苗张木

摘 要：采用冲击试验评定钢箱梁焊接工艺存在局限性，指出用裂纹尖端张开位移（CTOD）试验评定钢箱梁焊接工艺的优越性。介绍了焊接工艺CTOD断裂韧度评定的方法。针对港深西部通道香港段后海湾大桥钢箱梁焊接建造，运用英国标准BS7448对两项拟用焊接工艺进行CTOD试验评定。结果表明，埋弧自动焊工艺焊接接头的CTOD断裂韧度较高，该工艺可以直接用于钢箱梁焊接施工；而焊条电弧焊工艺焊接接头的CTOD断裂韧度较低，经扫描电子显微镜断口分析和X射线分析，发现其原因是焊缝中心存在气泡、微裂纹、夹杂物和硫等有害元素。试验评定结果为港深西部通道香港段后海湾大桥钢箱梁焊接质量控制提供了依据。

关键词：钢箱梁；裂纹尖端张开位移；CTOD；断裂韧度；焊接接头

中图分类号：TB302.3 文献标识码：A 文章编号：0253－360X(2006)04－077－04

0 序 言

韧度是材料在断裂前所经历的弹塑性变形过程中吸收能量的能力，是强度和塑性的综合表现。焊接接头中焊缝和热影响区的韧度往往低于其母材。母材钢板越厚，焊接接头韧度降低越明显。

目前国内对钢箱梁的焊接接头的韧度评定中，主要采用冲击试验，这样做有较大局限性。首先，冲击韧性本质上是一个衡量焊接接头抗冲击能力的力学量，不能全面反映焊接接头的真实韧度。其次，冲击试验的试样取样受到限制。按有关冲击试验规范[1]，冲击试验的标准试样尺寸是10 mm×10 mm×55 mm。因此，对于厚度大于10 mm的钢板的焊接接头，冲击试验的结果就不能代表整个焊接接头的韧度。再者，材料表现为韧性断裂还是脆性断裂，不仅取决于材料本身，还与材料所受应力状态有关。韧性材料在三向拉应力状态下，表现为脆性断裂，而脆性材料在三向压应力状态下，表现为韧性破坏。冲击试样的局部取样，改变了试样所处的应力状态，就不能模拟原焊接接头的应力状态。随着桥梁跨度的不断增加，钢箱梁所用钢板越来越厚，这个问题越突出。

港深西部通道是连接香港和深圳两地的第四条跨界通道，其中位于香港段的后海湾大桥的钢箱梁，宽39 m，高4.2 m，中腹板厚度达到65 mm，它是目前国内钢板厚度最大的钢箱梁。因此，对梁段匹配制造和工地装焊所用的焊接工艺，仅仅进行常规冲击试验还不够，必须用CTOD试验对其焊缝和热影响区的韧度进行有效控制。

1 焊接接头CTOD试验

1.1 母材

钢箱梁母材为日本产的S355ML热轧钢板，板厚65 mm，最大碳当量为0.45%，其化学成分见表1。主要力学性能参数屈服强度 R_{eL}＝423 MPa，抗拉强度 R_m＝526 MPa。

1.2 焊接工艺

钢箱梁常用埋弧自动焊（SAW）和焊条电弧焊（SMAW）。文中编制了两种拟用焊接工艺，它们均为双V形坡口，其最低预热温度为60 ℃。最高层间温度为300 ℃，见表2及表3。

表1 S355ML钢化学成分（质量分数，%）

Table 1 Chemical composition of S355ML steel

C	Si	Mn	P	S	Cu	Ni	Cr	Mo	V	Nb	N	Ti
0.09	0.27	1.45	0.011	0.002	0.08	0.05	0.01	0.002	0.001	0.12	0.38	0.12

收稿日期：2005－10－12

表 2 埋弧自动焊(PWPS017)工艺参数

Table 2 Parameter of submerged arc welding (PWPS017)

焊道序号	焊丝	直径 D/mm	电流 I/A	电压 U/V	极性	送丝速度 v_1/(m·min^{-1})	行走速度 v_2/(mm·min^{-1})	热输入 E/(kJ·mm^{-1})
1	H10Mn2G (BZJ116—97)	5.0	644~756	28~32	DC+	1.2~1.4	353~414	3.3
其它		5.0	671~788	28~32		1.2~1.4	342~403	3.5
盖面焊		5.0	651~761	28~32		1.2~1.4	353~414	3.3

表 3 焊条电弧焊(PWPS016)工艺参数

Table 3 Parameter of shielded metal arc welding (PWPS016)

焊道序号	电焊条	直径 D/mm	电流 I/A	电压 U/V	极性	行走速度 v_2/(mm·min^{-1})	热输入 E/(kJ·mm^{-1})
1	QSH—J507Ni	3.2	100~120	20~22		50~75	1.8
其它	(AWSA5.5	4.0	120~150	22~26	DC+	75~100	1.8
盖面焊	E7015—G)	4.0	120~150	22~26		75~100	1.8

1.2.1 埋弧自动焊(编号:PWPS017)

(1) 焊接过程:埋弧自动焊 SAW(DC+)。

(2) 焊丝:H10Mn2G (BZJ116—97)。

(3) 焊接位置:平焊。

1.2.2 焊条电弧焊(编号:PWPS016)

(1) 焊接过程:焊条电弧焊 SMAW(DC+)。

(2) 电焊条:QSH-J507Ni(AWS A5.5E7015—G)。

(3) 焊接位置:立向上焊接。

1.3 试样制备

按英国标准 BS7448—1[2] 和英国标准 BS7448—2[3] 制备三点弯曲试样。试样长度垂直于焊缝方向。焊缝(WP)试样横截面为 $B\times 2B$ 型的矩形(B 是试样厚度,$2B=W$ 是试样宽度),裂纹开在焊缝中心,取向为 NP 方向[3];热影响区(HAZ)试样横截面为 $B\times B$ 型,裂纹开在熔合线上,取向为 NQ 方向[3],裂纹尖端位置离开熔合线的距离不能超过0.5 mm。

1.4 CTOD 试验

按文献[2,3]的规范程序进行 CTOD 试验。断口有效性检验都符合规范要求。根据试验中测得的有关数据,按下式计算 CTOD 值[2],即

$$\delta=\left[\frac{FS}{BW^{1.5}}\times f\left(\frac{a_0}{W}\right)\right]^2\frac{(1-\mu^2)}{2\sigma_s E}+\frac{0.4(W-a_0)V_p}{0.4W+0.6a_0+Z}, \tag{1}$$

式中:δ为裂纹尖端张开位移(CTOD);F 为施加的载荷;S 为三点弯曲试样的跨度;B 为试样厚度;W 为试样宽度;μ 为泊松比;E 为弹性模量;α_0 为原始裂纹长度;f 为三点弯曲试样(α_0/W)的函数;V_p 为裂纹嘴张开位移的塑性分量;R_{eL} 为屈服强度;Z 为刀口厚度。

母材、埋弧自动焊和焊条电弧焊试样的主要参数及特征 CTOD 值分别列于表 4 和表 5。试验平均温度为 15 ℃,在该温度下母材试样(C—J01—1)的最大载荷 CTOD 值 $\delta_m=0.940$ mm[4]。

表 4 PWPS017 工艺试样主要参数及特征 CTOD 值

Table 4 CTOD values and parameters of specimen of craft PWPS017 (15℃)

试样编号	裂纹位置	力学性能	试样厚度 B/mm	试样宽度 W/mm	裂纹长度 a_0/mm	a_0/W	最大载荷 δ_m/mm	平均值 $\bar{\delta}_m$/mm
C—ZB01—2	焊缝 (WP)	R_{eL}=396.78MPa R_m=482.05MPa E=209.31GPa μ=0.262	54.00	107.73	54.25	0.50	0.750	0.714
C—ZB01—3			54.13	108.09	54.31	0.50	0.763	
C—ZB01—4			54.00	108.13	54.17	0.50	0.630	
C—ZB01—2	热影响区 (HAZ)	R_{eL}=420.84MPa R_m=520.04MPa E=213.30GPa μ=0.269	54.07	54.06	26.84	0.50	1.083	1.586
C—ZB01—4			54.10	54.18	26.68	0.49	1.797	
C—ZB01—6			54.10	54.00	26.48	0.49	1.879	

表 5　PWPS016 工艺试样主要参数及特征 CTOD 值

Table 5　CTOD values and parameters of specimen of craft PWPS016(15℃)

试样编号	裂纹位置	力学性能	试样厚度 B/mm	试样宽度 W/mm	裂纹长度 a_0/mm	a_0/W	脆性失稳 CTOD 值 δ_u/mm	平均值 $\bar{\delta}_u$/mm
C—SB01—1	焊缝（WP）	R_{eL}=518.39MPa R_m=612.68MPa E=210.59GPa μ=0.267	54.00	108.17	54.91	0.51	0.243	0.351
C—SB01—4			54.14	107.88	54.98	0.51	0.605	
C—SB01—6			54.12	108.11	54.85	0.51	0.206	

1.5　工艺评定结果

由表 4 可见，埋弧自动焊工艺（PWPS017）焊缝 CTOD 平均值为 0.714 mm，最小值为 0.630 mm。热影响区 CTOD 平均值为 1.586 mm，最小值为 1.083 mm，甚至大于母材 CTOD 值（δ_m=0.940 mm），这主要是热影响区晶粒细化从而提高了韧度。参考有关钢结构规范[5~7]和同类钢结构设计许可值[4,8]，将 CTOD 允许值定为 0.25 mm[9]。上述埋弧自动焊（PWPS017）接头 CTOD 值较大，超过了允许值（0.25 mm），该工艺可用于钢箱梁建造。

2　CTOD 试样断口分析

表 5 中焊条电弧焊（PWPS016）焊缝 CTOD 最小值仅为 0.206 mm，小于允许值（0.25 mm），韧度不够，该工艺需要调整修订。

对母材、PWPS017 工艺焊缝和 PWPS016 工艺焊缝的 CTOD 试样断口的电镜试样观察表面微区组织、成分。

图 1 是母材试样（C—J01—1）断口电镜照片，显示有较多等轴韧窝。它们是由垂直于断口总平面的正应力所产生的空洞聚集所形成的。有些韧窝中含有颗粒，用 X 射线分析方法分析颗粒的成分如下：铁 87.92%、锰 2.63%、硅 3.98%、铝 5.49%，还有少量的钨。韧窝是韧性断裂的主要电子金相特征。

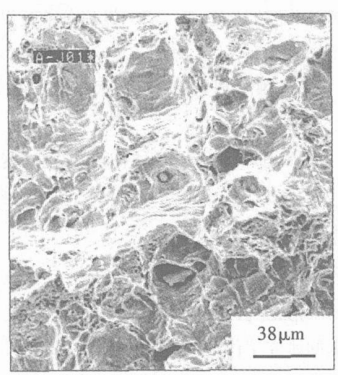

图 1　母材电镜照片

Fig. 1　SEM photograph of basic metal

图 2 为埋弧自动焊（PWPS017）焊缝试样断口上的韧窝群。未发现有解理台阶。存在一些颗粒，能谱分析表明这些颗粒的成分是铁、锰等基体，还有硅、铝和钙等。

图 3 是焊条电弧焊（PWPS016）焊缝断口，有许多解理台阶夹杂物的成分是 Cl、Ca、K、Si 和 S 等。气泡和夹杂物等产生应力集中，降低焊缝韧度。同时，硫是有害杂质，它容易使焊缝金属产生结晶裂纹，从而影响焊缝韧度。

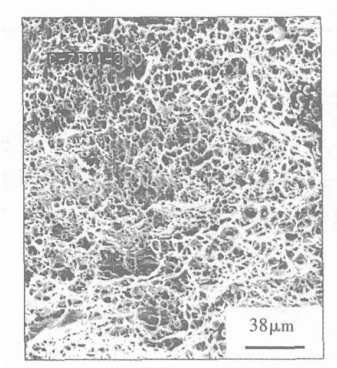

图 2　自动埋弧焊断口

Fig. 2　fractography of PWPS017

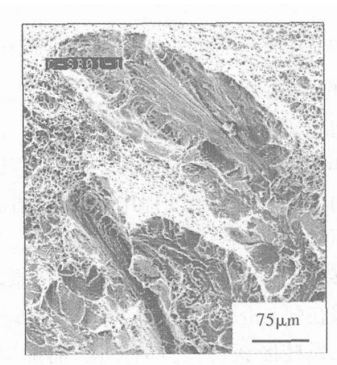

图 3　焊条电弧焊断口

Fig. 3　fractography of PWPS016

4 结 论

(1) 依据英国标准规范 BS7448, 对两种焊接工艺厚钢板接头, 进行了常温 CTOD 断裂韧度试验。表明埋弧自动焊的焊缝和热影响区的断裂韧度较高, 可以直接用于钢箱梁的焊接施工; 而焊条电弧焊工艺的焊缝的断裂韧度过低, 原因是存在含有硫元素的夹杂物、气泡和微裂纹。

(2) 试验结果为保证港深西部通道后海湾大桥钢箱梁的建造质量提供了依据, 并为改进焊条电弧焊工艺提供了思路。

参考文献:

[1] GB2649— 1989. 焊接接头机械性能试验取样方法[S].

[2] BS7448Part1— 1991. Fracture Mechanics Toughness Test [S].

[3] BS7448Part2— 1997. Fracture Mechanics Toughness Test [S].

[4] 苗张木. 厚钢板焊接接头韧度CTOD 评定研究[D]. 武汉: 武汉理工大学. 2005.

[5] DET Norske Veritas. Offshore Standard DNV— OS—C401: 2001. Fabrication and Testing of Offshore Structures[S].

[6] DET Norske Veritas. Offshore Standard DNV— OS— F101: 2000. Submarine Pipeline Systems[S].

[7] American Petroleum Institute. Recommended practice 2Z: 1998. Recommended Practice for Preproduction Qualification for Steel Plates for Offshore Structures[S].

[8] 杨新歧, 王东坡, 李小巍, 等. 海洋石油平台焊接接头大型CTOD 试验[J]. 焊接学报, 2002, 23(4): 48— 52.

[9] 苗张木, 陶德馨, 杨荣英. 焊接接头韧度CTOD 评定的适用性与允许值研究[J]. 机械强度, 2006, 28(1): 150— 154.

作者简介: 苗张木, 男, 1957 年 11 月生, 博士, 副教授。主要研究方向: 结构强度、疲劳与断裂、母材、焊接接头CTOD 试验等, 发表论文 20 多篇。

Email: zmmiao@mail.whut.edu.cn

[上接第 63 页]

在自调节作用, 在焊芯间距较小时, 弧柱热量对焊芯的熔化不一致的补偿作用较强, 双电极焊条两焊芯能保证同速熔化, TESAW 电弧稳定燃烧。

3 结 论

(1)由于电弧焊中阴、阳极产热一般不同, 在TESAW 焊条燃烧过程中存在一定的双电极焊条两芯熔化不一致现象, 此现象还受焊条类型, 焊接电流等因素的影响。

(2)双电极焊条两芯熔化一致的充分条件为: $U_{阳效}=U_{阴效}$ 或 $U_{阴}=U_{阳}+2\times(\frac{3}{2}kT+\varphi)$; 若此条件不满足, 则两焊芯熔化不一致; $U_{阳效}$ 与 $U_{阴效}$ 差值越大则焊芯熔化不一致程度越大。

(3)双电极焊条单弧焊电弧对两焊芯熔化存在自调节作用, 即电弧燃烧过程中两焊芯端部在电弧中的长度不等, 两焊芯仍能保持等速熔化, 使电弧燃烧过程能够稳定进行。电弧自调节作用原理是由于两焊芯端部在弧柱区的长度不同, 伸入弧柱区中较长的焊芯从弧柱区获得更多的热量, 而加快其熔化, 从而起到电弧的自调节作用。一般随焊芯间距的减小及焊接电流的增大, 电弧自调节作用增强。

参考文献:

[1] Quigley M B C. Physics of the welding arc[J]. Welding &Metal Fabrication, 1977, 45(10): 619— 626.

[2] 中国机械工程学会焊接学会. 焊接手册 ——焊接方法及设备(第二版)[M]. 北京: 机械工业出版社, 2002.

[3] Ter Berg J, Larigaldie A. Melting rate of coated electrodes[J]. Welding Journal, 1952, 32(5): 268s— 271s.

[4] Pokhodnya I K, Gorpenyuk V N, Milichenko S S, *et al*. Metallurgy of arc welding. Vol. 1: Arc processes and electrode melting[M], Rieckansky Science Publishing Co., Cambridge, U.K. 1991. 173 ~ 222.

[5] 姜焕中. 电弧焊及电渣焊(第 2 版)[M]. 北京: 机械工业出版社, 1995.

[6] 邹增大, 曲仕尧, 王新洪, 等. 双芯焊条及单弧焊接工艺[P]. 中国发明专利: CN ZL01115103. X, 2004— 04— 09.

[7] 邹增大, 韩 彬, 曲仕尧, 等. 双电极焊条单弧焊电弧特性研究[J]. 焊接学报, 2004, 25(1): 5— 7.

[8] 王 宝. 焊接电弧物理与焊条工艺性设计[M]. 北京: 机械工业出版社, 1998.

[9] 韩 彬, 邹增大, 李立英, 等. 双电极钛钙型碳钢焊条焊芯间距对焊接工艺及电弧形态的影响[J]. 石油大学学报(自然科学版), 2004, 28(4): 94— 96.

作者简介: 韩 彬, 男, 1973 年 9 月出生, 工学博士, 讲师。从事新材料及连接技术的研究工作, 发表论文 20 篇。

Email: hlhzhjh@hdpu.edu.cn

tractions of welding easier. In addition, the feature-based modeling system provides the robotic welding off-line programming system with adequate information and is successfully applied.

Key words: geometric model of weld; feature extraction of welding; list structure of features; feature-based modeling; SolidWorks

Melting characteristic of twin electrode single arc welding II. Self-regulating effect of arc on two cores melting HAN Bin[1], ZOU Zeng-da[2], QU Shi-yao[2] (1. School of Mechanical and Electronic Engineering, Petroleum University of China, Dongying 257061, Shandong, China; 2. School of Materials Science and Engineering, Shandong University, Jinan 250061, China). p61—63, 80

Abstract: Two cores melting speed can keep consistence is very important for twin electrode single arc welding to be stabilized. The melting consistency of two cores is influenced by electrode type, welding current etc. The sufficient condition of two cores melting coincidence is the effective anode drop equal to the effective cathode drop, the more the difference of two values the more the melting inconsistent degree. The arc has a self-regulating effect on melting of two cores, that is, during the arc burning, even if the ends of two cores have different length in the arc, two cores can keep uniformly melting speed, and the arc can stably burn. The principle of the self-regulating effect is that different heat production of cathode and anode make two cores length in the arc different. The longer weld core stretching into the arc column gets more heat from the arc column to accelerate its melting. In general, the self-regulation effect of arc increases with the reducing of two-core span and increasing of welding current.

Key words: twin electrode; single arc welding; two cores melting; self-regulation effect

Submerged arc welding wire matched with X80 pipeline steel ZHANG Min, YAO Cheng-wu, FU Chong, LV Zhen-lin (School of Material Science and Engineering, Xi'an University of Technology, Xi'an 710048, China). p64—68

Abstract: By analyzing the influence of the microstructure for weld deposited metal of high strength low-alloy steel on mechanical properties, the compound microstructure deposit with mainly the acicular ferrite (AF) and a small quantity of the granular bainite (GB) was applied to the welding wire for X80 pipeline steel. Based on the driving force concept of microstructure transformation, and combined with the acicular ferrite nucleated mechanism at nonmetallic inclusions and microalloy toughness theory, the Mn—Ni—Mo—Ti—B alloy was selected to study the welding wire of X80 pipeline steel. The results of experiments show that the weld deposited metal will fulfil the demands of strength and toughness and low-temperature toughness by choosing and controlling alloy elements rationally, and the developed 1# welding wire can be used for X80 pipeline steel.

Key words: X80 pipeline steel; submerged arc welding; low temperature toughness; acicular ferrite; inclusion

Effect of TiO_2 on detachability of stainless steel electrode LI Ping, MENG Gong-ge (Harbin University of Science & Technology, Harbin 150080, China). p69—72

Abstract: With uniform design method, tooking the coating ingredients as independent variables and slag detachability as the target function in the formula and usability test, the effects of coating components on the detachability of stainless steel electrode were studied. Based on the calculates and analysis result, the two bigger effective supplementary materials-rutile and the powder of TiO_2 were studied. When they (mainly TiO_2) increase, the microscopic structure in the slag will form branchlike or the stronger directive frame-like structure. The white fir-tree crystal phase gets more and the detachability turns better, as the branches get longer, the branching area bigger and denser.

Key words: uniform design; mechanism; detachability; microstructure

3D finite element simulation on stress-strain distributions in all position root butt welding of pip HUANG Si-luo[1,2], XUE Yong[1], ZHANG Jian-xun[1], Chen Zong-qiang[2] (1. Xi'an Jiaotong University, Xi'an 710049, China; 2. Maoming Petrochemical Machinery Plant, Maoming 525024, Guangdong, China). p73—76, 84

Abstract: Based on thermal—elastic—plastic theory, a 3—D finite element model of root butt welding of SA335 P91 steel pipe was carried out with ANSYS software. Using moving heat source, the transient temperature field and welding stress-strain field in root butt welded joint of a pipe were analyzed. Moreover, the distributions of axial and hoop transient stresses to close the two-half seam joint were investigated. The calculation results show that the axial and hoop stresses at the keyhole center are tensile, specially, the edge stress effect is remarkable where the hoop stresses are stronger than the axial ones, and how the holding time of heat source in the keyhole and the welding current influences the distribution of stresses and strain during the high temperature solidification is also discussed.

Key words: SA335 P91 steel pipe; numerical simulation; stress-strain field; solification cracking

Evaluation of welding procedure specification with crack tip opening displacement in steel box beam MIAO Zhang-mu[1], WU Wei-guo[1], TAO De-xin[2], XIE Zhi-hua[3] (1. School of Transportation, Wuhan University of Technology, Wuhan 430063 China; 2. School of Logistics, Wuhan University of Technology, Wuhan 430063 China; 3. The Seventh Engineering Company Ltd., Of China Railway Major Bridge Bureau, Jiujiang 332004, Jiangxi, China). p77—80

Abstract: The limitations and problems of evaluation of welding procedure specification (WPS) of steel box beam with impact test were analyzed. It is necessary to use the crack tip opening displacement (CTOD) test to evaluate WPS of steel box beam. The CTOD

test was presented. Two WPS used for the fabrication of steel box beam of back-gulf Bridge in Hong Kong—Shenzhen Western Corridor was designed and evaluated with CTOD test according to BS7448. The results are as follows: 1) The values of CTOD fracture toughness in welded joints of submerged arc welding (SAW) are higher. The welding procedure specification of SAW can be directly applied to the fabrication of steel box beam. 2) The values of CTOD in welded joints of shielded metal arc welding (SMAW) are lower. Hence the welding procedure specification of SMAW should be amended. It is found by scanning electron microscope that there are gas holes and micro-cracks and inclusion and harmful sulphur in the welding position.

Key words: steel box beam; crack tip opening displacement; toughness; welded joints

Development and property analysis of ultra-low carbon self-shielded flux-cored wire with nitride solid solution strengthening

WANG Qing-bao, LIU Jing-feng, SHEN Feng-gang (Welding Research Institute, Central Research Institute Building & Construction, MCC, Beijing 100088, China). p81—84

Abstract: Ultra-low-carbon 00Cr13Ni4MoN series self-shielded flux-cored wires using nitrogen solid solution strengthening were developed. The wires have excellent welding usability and mechanical properties. The microstructure of the deposited metal is nearly single martensite, which possesses temper-resistant softening property, toughness and resistance to wear.

Key words: self-shielded flux-cored wire; welding usability; nitride solid solution strengthening

High temperature oxidation behavior of arc sprayed duplex aluminum bronze based coatings

ZHANG Zhong-li[1], LI De-yuan[1], ZHANG Nan-nan[1], XIAO Xuan[2] (1. School of Material Science and Engineering, Shenyang University of Technology, Shenyang 110023, China; 2. Liaoning Physical and Chemical Analysis Center, Shenyang 110015, China). p85—88

Abstract: The performance and effectiveness of arc-sprayed duplex coatings on mild steel was evaluated. The duplex coating structure is comprised of an inner aluminum bronze layer and an outer layer of aluminum 0.1—0.2 mm. Cyclical oxidation test, each lasting 12 hours, was performed in air at 900 ℃ for ten times. The results demonstrated that the coating had a better oxidation resistance than single aluminum bronze coating. The application of aluminum layer benefits the formation of a thick alumina-rich protective layer on coating surface and the sealing of the pores of coatings at elevated temperature. After one cyclical oxidation test, a continuous Al_2O_3 layer was formed along the interface coating/substrate, which did not make the coating adhesion degraded. The composite coatings provided steel substrate with a good high temperature protection. The composite coating would be a potential candidate for protecting steel substrate at high temperature.

Key words: arc spraying; high temperature oxidation; aluminum bronze; duplex coatings

Influence of air-arc cutting on initial stress fields

HU Jun-feng[1], YANG Jian-guo[1], FANG Hong-yuan[1], CHEN Wei[1], LI Guang-min[1,2] (1. State Key Laboratory of Advanced Welding Production Technology, Harbin Institute of Technology, Harbin 150001, China; 2. Bohai Shipbuilding Heavy Industry Co. Ltd, Huludao 125004, Liaoning, China). p89—92

Abstract: The influence the stress fields of air-arc cutting for 10Ni5CrMoV steel plates are simulated using finite element method and the simulating results are according well with the experiments results. The stress fields of air-arc cutting for 10Ni5CrMoV steel plates and the mechanics of influences on initial stress fields of air-arc cutting are studied further. The results show that the stable stress fields of air-arc cutting are similar to that of the butt plates welding. There are tensile stresses near the groove and then they turn low gradually, and finally the transversal stresses approach zero stress while the longitudinal stress change to compressive stress. The influence of air-arc cutting on the initial stress fields contain two aspects: 1) the stresses near the groove are released because of the metal materials wiped away; 2) the thermal function of the arc made a higher tensile stress existed near the groove, and it is more intense than the former.

Key words: air-arc cutting; finite element method; initial stress fields; stress fields

Boundary element math model of welding residual stresses determination

DENG Hua-ling[1,2], MA Hang[3] (1. China University of Petroleum (Rast China), Dongying 257061, Shangdong, China; 2. Shandong Electric Power Research Institute, Jinan 250002, China; 3. Shanghai University, Shanghai 200072, China). p93—96

Abstract: There is a definite correlation between the welding residual stresses and deformations, which can be connected by the incompatible strains formed in the welding process. Based on the initial welding strain, a math model of 2D welding residual stresses determination was deduced through direct boundary clement method. If the value of the initial welding strain was given, and in light of the measured boundary displaces, all the unknown displacemcnts and traction at the boundary could be calculated by using the boundary integral equation. Thereby, by using the model, the residual stresses of the weld structure could be solved. The stresses at the boundary can be calculated by the physical equation and the geometric equation according to the correlation between the stresses and the traction at the boundary. The feasibility of the model was verified through a concrete computing instance.

Key words: welding deformation; residual stresses; initial strain; boundary element method; math model

Study on C/S interface in Fe based high carbon Nb—Ti—V alloyed surfacing welding layer

ZHANG Yuan-bin[1], REN Deng-